Supporting Information

Witte et al. 10.1073/pnas.1009314107

SI Materials and Methods

Mice, Skeletal Preparations. *Ror2*^{W749X}, *Ror2*^{TMLacZ}, and *Ihh*^{E95K} mouse lines were described previously (1–3). *Ror2*$^{+/-}$ mice (4) were provided by Y. Minami (Kobe University, Kobe, Japan), *Ihh*$^{+/-}$ mice (5) were provided by A. P. McMahon (Harvard University, Boston, MA). *Axin2*^{LacZ} Wnt reporter mice (6) were obtained from W. Birchmeier (Max Delbrück Center for Molecular Medicine, Berlin, Germany). Genotyping was performed using DNA prepared out of tailtip or amnion samples according to standard procedures; for primer sequences and PCR conditions see respective references. Skeletal preparations were performed according to standard protocols (7). All animal experiments were carried out in compliance with legal requirements of the European Union.

Histology, In Situ Hybridization, Immunohistochemistry. Whole mount in situ hybridizations on forelimbs as well as section in situ hybridizations on 7-μm paraffin sections were performed as previously described (8). The following probes were used: *Bmpr1b* (9), *Bmp4* (10), *Collagen II alpha 1* (7), *Gli1*, *Ihh*, and *Patched1* (6, 11), *Gdf5* and *Runx2* (12), and *Sox9* (13).

Other probes were amplified using the following primers (forward/reverse):

Nmyc: CATCCATCAGCAGCACAACT/AAATGTGCAAAGTGGCAGTG
Itf2: TGAGCTATCCATCCCACTCCTC/TGTCTTGCAGGTTCTCATCGCC

LacZ staining was performed on whole-mount and cryosection samples as described previously (14). Mutant and WT specimens used for comparison were derived from the same litters and processed in parallel.

Immunohistochemistry was performed on 7-μm paraffin sections. Sections were deparaffinized using xylene and rehydrated in a descending series of ethanol concentrations. Antigen retrieval was performed using citrate buffer or high-pH buffer (Dako). Slides were boiled twice for 3 min and allowed to cool down to room temperature for 30 min. After permeabilization with 0.2% Triton X-100 in PBS for 15 min and blocking with 5% normal goat serum in PBS, primary antibody incubation was performed at 4 °C in 5% normal goat serum in PBS overnight. Detection with fluorescence-conjugated secondary antibody (Molecular Probes, Invitrogen) was performed at room temperature for 1 h. Primary antibodies, dilution, and retrieval were as follows: antiactivated β-catenin (Upstate, 1:100, high-pH), anti-BrdU (Roche, 1:20, citrate) anti-phosphoSMAD1/5/8 (Cell Signaling, 1:200, high-pH), anti-SOX9 (Santa Cruz Biotechnology, 1:50, citrate), anti-TCF7L2 (Upstate, 1:100, high-pH), activated (cleaved) caspase 3 (Cell Signaling, 1:200, citrate). For phospho-SMAD staining, additional biotinyl tyramid signal amplification was performed according to the manufacturer's protocol (Perkin-Elmer). Sample examination was done with an AxioVert 200 fluorescence microscope, ApoTome technology, and AxioVision software (Zeiss).

BrdU Pulse-Chase Labeling. Mice were injected i.p. with 200 μg BrdU per gram body weight. After 1 h incorporation was blocked by injection of a 30-fold excess of thymidine (15, 16). After an additional 10 h, mice were killed and embryos processed for immunhistology on paraffin sections. Statistical analysis was performed by counting BrdU/SOX9-positive cells in relation to SOX9-positive cells on four sections for each WT and mutant specimen. The experiment was repeated three times; mean values from the three experiments were averaged and an SE calculated from the individual SDs.

Micromass Cultures. Mouse micromass cultures were prepared at embryonic day 12.5 (E12.5). Limbs were collected in warm PBS and digested for 15 min at 37 °C with 3 mg/mL dispase. After washing, cells were isolated from the limb buds by digestion with 0.1% collagenase type Ia, 0.1% trypsine, and 5% FCS. Micromass cultures were plated at a density of 3.6×10^7 cells in a 10-μL drop. After 2 h of adhesion, 1 mL of medium (DMEM-F12, 10% FCS, 1% L-glutamine, and 1% Pen/Strep) was added and refreshed every 2 d. Alcian blue staining and quantification was performed as previously described (17).

1. DeChiara TM, et al. (2000) Ror2, encoding a receptor-like tyrosine kinase, is required for cartilage and growth plate development. *Nat Genet* 24:271–274.
2. Raz R, et al. (2008) The mutation ROR2W749X, linked to human BDB, is a recessive mutation in the mouse, causing brachydactyly, mediating patterning of joints and modeling recessive Robinow syndrome. *Development* 135:1713–1723.
3. Gao B, et al. (2009) A mutation in Ihh that causes digit abnormalities alters its signalling capacity and range. *Nature* 458:1196–1200.
4. Takeuchi S, et al. (2000) Mouse Ror2 receptor tyrosine kinase is required for the heart development and limb formation. *Genes Cells* 5:71–78.
5. St-Jacques B, Hammerschmidt M, McMahon AP (1999) Indian hedgehog signaling regulates proliferation and differentiation of chondrocytes and is essential for bone formation. *Genes Dev* 13:2072–2086.
6. Lustig B, et al. (2002) Negative feedback loop of Wnt signaling through upregulation of conductin/axin2 in colorectal and liver tumors. *Mol Cell Biol* 22:1184–1193.
7. Mundlos S (2000) Skeletal morphogenesis. *Methods Mol Biol* 136:61–70.
8. Stricker S, et al. (2006) Cloning and expression pattern of chicken Ror2 and functional characterization of truncating mutations in Brachydactyly type B and Robinow syndrome. *Dev Dyn* 235:3456–3465.
9. Baur ST, Mai JJ, Dymecki SM (2000) Combinatorial signaling through BMP receptor IB and GDF5: Shaping of the distal mouse limb and the genetics of distal limb diversity. *Development* 127:605–619.
10. Bitgood MJ, McMahon AP (1995) Hedgehog and Bmp genes are coexpressed at many diverse sites of cell-cell interaction in the mouse embryo. *Dev Biol* 172:126–138.
11. Vortkamp A, et al. (1996) Regulation of rate of cartilage differentiation by Indian hedgehog and PTH-related protein. *Science* 273:613–622.
12. Stricker S, Fundele R, Vortkamp A, Mundlos S (2002) Role of Runx genes in chondrocyte differentiation. *Dev Biol* 245:95–108.
13. Healy C, Uwanogho D, Sharpe PT (1999) Regulation and role of Sox9 in cartilage formation. *Dev Dyn* 215:69–78.
14. Lobe CG, et al. (1999) Z/AP, a double reporter for cre-mediated recombination. *Dev Biol* 208:281–292.
15. Haaf T (1996) High-resolution analysis of DNA replication in released chromatin fibers containing 5-bromodeoxyuridine. *Biotechniques* 21:1050–1054.
16. Schmahl J, Eicher EM, Washburn LL, Capel B (2000) Sry induces cell proliferation in the mouse gonad. *Development* 127:65–73.
17. Woods CG, et al. (2006) Mutations in WNT7A cause a range of limb malformations, including Fuhrmann syndrome and Al-Awadi/Raas-Rothschild/Schinzel phocomelia syndrome. *Am J Hum Genet* 79:402–408.

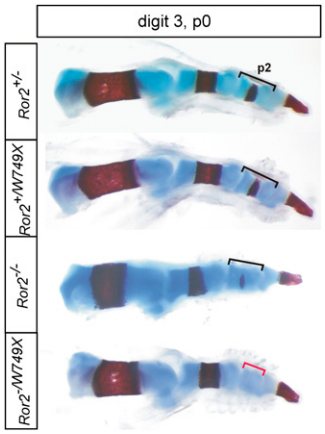

Fig. S1. Gain-of-function of the Ror2W749X allele. Ror2+/W749X mice were crossed to Ror2+/- mice. Ror2-/- mutants (1) exhibit severe skeletal defects but no BDB1-like phenotype, because all phalangeal condensations are present, albeit shortened, which is due to a failure of growth plate organization and chondrocyte maturation in these mutants (2). Skeletal preparations of middle fingers (digit 3) of newborn mice stained with Alcian blue (cartilage) and alizarin red (bone) are shown. Ror2+/W749X and Ror2+/- heterozygote animals have normal phalanges, whereas the Ror2-/- mutant has a slightly shortened middle phalanx (p2) concomitant with the delayed cartilage maturation and ossification seen in all long bones. The Ror2-/W749X compound mutant, however, shows a pronounced shortening of p2 that is markedly stronger than the Ror2-/- phenotype, indicating a gain of function for the ROR2-W749X protein, which, however, is masked by the presence of one WT Ror2 allele in Ror2+/W749X mice.

1. Takeuchi S, et al. (2000) Mouse Ror2 receptor tyrosine kinase is required for the heart development and limb formation. *Genes Cells* 5:71–78.
2. Schwabe GC, et al. (2004) Ror2 knockout mouse as a model for the developmental pathology of autosomal recessive Robinow syndrome. *Dev Dyn* 229:400–410.

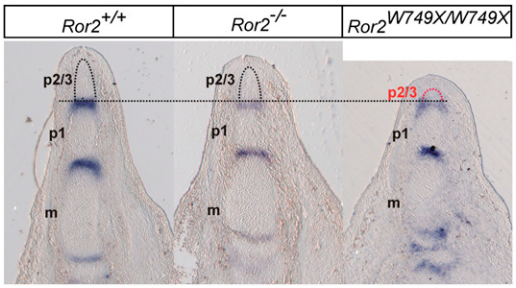

Fig. S2. The distal elongation defect is specific to the *Ror2*$^{W749X/W749X}$ mutant. Longitudinal sections (proximal is at the bottom, distal at the top) were labeled for the joint marker *Gdf5*. Pictures were arranged placing the p1-p2/3 joint on the same level (dotted line). Note that the defect in p2/3 elongation only occurred in the *Ror2*$^{W749X/W749X}$ mutant but not in the *Ror2*$^{-/-}$ mutant. m, metacarpal; p1, phalanx 1; p2/3, unseparated primordium of phalanges 2 and 3.

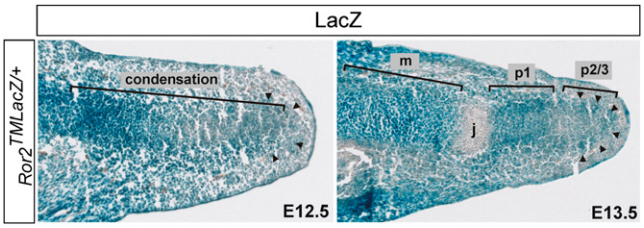

Fig. S3. Expression of ROR2 during digit outgrowth demonstrated by LacZ staining on longitudinal sections from *Ror2*$^{TMLacZ/+}$ embryos at E12.5 and E13.5. Proximal is left, distal is right. ROR2 is expressed in cartilage condensations and other mesenchymal tissues. Note that ROR2 shows enhanced expression in distal mesenchyme undergoing chondrogenesis (arrowheads), forming the condensation of the second and third phalanges at E13.5. j, joint; m, metacarpal; p1, condensation of phalanx 1; p2/3, unseparated primordium of phalanges 2 and 3.

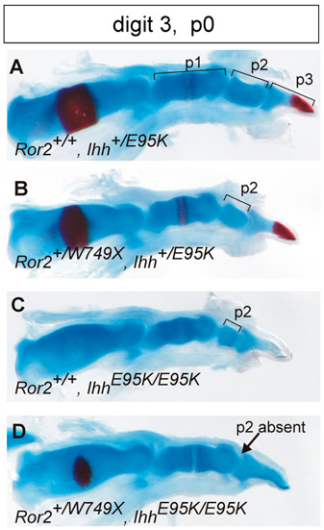

Fig. S4. Genetic interaction of *Ror2*^{W749X} (BDB1 mutation) and *Ihh*^{E95K} (BDA1 mutation). Skeletal preparations of digits 3 from newborn mice (p0) of the allelic combinations indicated were stained with Alcian blue (cartilage) and Alizarin red (bone). Note that the compound heterozygotes show increased phenotypic severity compared with the *Ihh*$^{+/E95K}$ mutant (*A* and *B*). On the homozygous *Ihh*$^{E95K/E95K}$ background (*C*), addition of one *Ror2*^{W749X} allele caused absence of the middle phalanx (p2), thus phenocopying *Ror2*$^{W749X/W749X}$ mice (*D*).

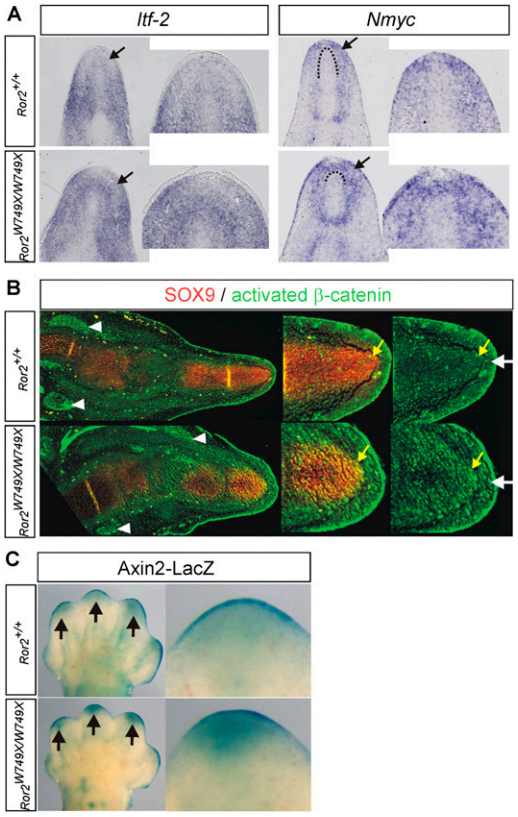

Fig. S5. Ectopic activation of the Wnt/β-catenin pathway in the distal mesenchyme of Ror2W749X/W749X mice. (*A*) Section in situ hybridization shows up-regulation of canonical Wnt targets Itf-2 and Nmyc (1, 2) in distal mesenchyme (arrows, magnifications) of Ror2W749X/W749X mice. (*B*) Immunohistochemistry for SOX9 (green) and activated (dephosphorylated) β -catenin (red) show elevated levels of β-catenin in distal mesenchyme (white arrows) and especially cells undergoing chondrogenesis in Ror2W749X/W749X mice (note yellow staining for overlapping signal with SOX9; yellow arrows). Note the equal intensity of β-catenin staining in muscles between WT and Ror2W749X/W749X (arrowheads). (*C*) LacZ staining on whole-mount embryos from intercrossing the Ror2W749X line to the canonical Wnt reporter line Axin2LacZ demonstrates increased canonical pathway activity in distal mesenchyme (arrows) of Ror2W749X/W749X mutants.

1. Kolligs FT, et al. (2002) ITF-2, a downstream target of the Wnt/TCF pathway, is activated in human cancers with beta-catenin defects and promotes neoplastic transformation. *Cancer Cell* 1: 145–155.
2. ten Berge D, Brugmann SA, Helms JA, Nusse R (2008) Wnt and FGF signals interact to coordinate growth with cell fate specification during limb development. *Development* 135: 3247–3257.

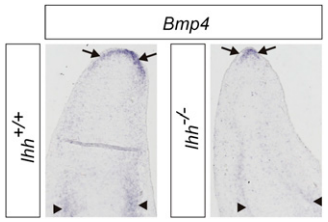

Fig. S6. Reduced expression of *Bmp4* in the distal mesenchyme of $Ihh^{-/-}$ mice shown by section in situ hybridization. In the WT, *Bmp4* is expressed in a broad domain in the distal undifferentiated mesenchyme; in the $Ihh^{-/-}$ mutant *Bmp4* expression is restricted to a small domain anterior to the growing phalanx (arrows). Note that the perichondral *Bmp4* expression is also decreased in $Ihh^{-/-}$ mutants (arrowheads).

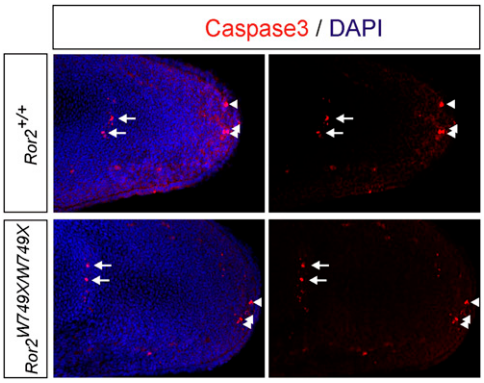

Fig. S7. Immunolabeling for activated caspase 3 shows no aberrant apoptosis in $Ror2^{W749X/W749X}$ mice at E13.5 compared with WT littermates. Apoptotic cells were detected in developing joints (arrows) and mesenchyme (arrowheads).